*Acta of Bioengineering and Biomechanics*
*Vol. 19, No. 2, 2017*

Original paper
DOI: 10.5277/ABB-00679-2016-04

# The influence of the cumulated deformation energy in the measurement by the DSI method on the selected mechanical properties of bone tissues

ANNA M. MAKUCH[1]*, KONSTANTY R. SKALSKI[1], MAREK PAWLIKOWSKI[2]

[1] Institute of Precision Mechanics, Warsaw, Poland.
[2] Institute of Mechanics and Printing, Warsaw University of Technology, Poland.

*Purpose*: The goal of the study was to determine the influence of DSI test conditions, i.e., loading/unloading rates, hold time, and the value of the maximum loading force on selected mechanical properties of trabecular bone tissue. *Methods*: The test samples were resected from a femoral head of a patient qualified for a hip replacement surgery. During the DSI tests hardness ($H_V$, $H_M$, $H_{IT}$) and elastic modulus (EIT) of trabecular bone tissue were measured using the Micro Hardness Tester (MHT, CSEM). *Results*: The analysis of the results of measurements and the calculations of total energy, i.e., elastic and inelastic ($W_{\text{total}}$, $W_{\text{elastic}}$, $W_{\text{inelastic}}$) and those of hardness and elasticity made it possible to assess the impact of the process parameters (loading velocity, force and hold time) on mechanical properties of bone structures at a microscopic level. *Conclusions*: The coefficient $k$ dependent on the $E_{IT}/H_{IT}$ ratio and on the stored energy ($\Delta W = W_{\text{total}} - W_{\text{elastic}}$) is a measure of the material reaction to the loading and the deformation of tissue.

*Key words*: *indentation, elasticity, trabecular bone, DSI method, energy deformation*

## 1. Introduction

In biomechanics the main research trends are related to experimental and numerical techniques of visualization and estimation of tissue material properties [15]. This research provides results that are very helpful in diagnosis and monitoring processes in clinical and rehabilitation procedures. Determination of material parameters of tissues, especially at a micro- or nanostructural level, is a significant difficulty in studies on tissues properties. The previous classical experimental studies on mechanical properties of tissue are based on static tests, i.e., tensile tests, compression tests, rotational tests, three-point bending and hammer or ultrasound tests [4]. Contemporary microstructural studies require integration of classical measurement methods with contactless ones or application of new methods, i.e., spot interferometry electronic method or digital image correlation [25]. A perspective direction in development of experimental tissue research is depth-sensing indentation (DSI), which is also applied in measurements of microhardness of thin layers.

The DSI method [18] is more and more applied to estimate mechanical properties of solids [22]. Its popularity results from the fact that it makes it possible to determine mechanical properties for materials of a relatively low volume without complicated sample preparation procedure. In addition, this method enables to determine all the needed values without optical measurement of the indenter impression. During indentation tests both force and displacement of the indenter are measured in the non-elastic and elastic domain [9]. Applying the DSI method one can determine Martens hardness (HM), the DSI hardness ($H_{IT}$) and elastic modulus ($E_{IT}$) according to the standard [19]. However, using Oliver–Pharr's method to

* Corresponding author: Anna Makuch, Institute of Precision Mechanics, ul. Duchnicka 3, 01-796 Warsaw, Poland. Tel: +48 609 832 133, e-mail: a.makuch1309@gmail.com

Received: June 23rd, 2016
Accepted for publication: November 22nd, 2016

evaluate the mechanical properties, it is necessary to take into account the nature of the tested material (isotropy, anisotropy, porosity, viscoelasticity, etc.). So far, a number of theoretical and experimental works devoted to the analysis of the influence of the process factors (hold time, loading/unloading velocity, maximum loading force, indentation depth) on the test results on metals [29], [10], plastics [17], [27] or composites [8] have been published. The dependence of hardness and elasticity parameters is particularly evident in the case of materials having rheological properties [9], [23]. The classical (contact) method should not produce correct results in the case of testing the materials dependent on time ([1] based on FEA). In addition, the loading/unloading velocity must also be taken into account. According to Tang et al., who evaluated PVDF, PMMA and epoxy resins in the study of nanoindentation using different loading forces, loading/unloading velocity, if the unloading is inflicted quickly enough, the viscoelastic effects can be overcome and the yield indicator becomes independent on the loading force, but dependent on the polymer structure and chemical composition. In the study of composite materials with complex internal structure, the applied loading and the indentation depth will significantly affect the resulting material parameters such as hardness and elasticity.

The DSI is also very useful in measurements of bone properties. A bone tissue is marked by a hierarchical and anisotropic structure [6]. However, the anisotropy of material properties is revealed only in the study of component elements at the level of trabecula: osteon, bone lamellae. The DSI and the Reference Point Indentation (RPI) were used to measure anisotropic behaviour of a bovine bone [5]. The aim of this study was a comparison of the results obtained from these two methods.

Katsamenis et al. [14] investigated mechanical behaviour of a cortical bone from a human femur. The study was made at three levels: osteonal, microstructural and tissue, using nanoindentation, the RPI and a fracture toughness experiment. The authors show that bone's fracture toughness and crack growth resistance at a tissue level are correlated with mechanical properties at micro- and osteonal levels. Jenkins et al., [11] carried out a study on the optimization of testing parameters based on RPI measurement. The RPI was applied to a bovine bone (femoral midshaft) and a human bone (femoral heads and a neck). Coutts et al., [3] is used the RPI as a new clinical tool to aid the diagnosis of osteoporosis. This testing could improve the understanding of bone mechanical properties. Indentations were made on human, bovine, porcine and rat femurs along three axes.

Performing the DSI tests on osteons of a cortical bone or trabeculae of a cancellous bone mechanical properties of those bone tissues at nano- and micro-levels can be established [16]. In the paper the results of a series of the DSI tests performed on a cancellous bone are presented. The indentations were made on trabeculae and the areas where two or more trabeculae connect with each other. The characteristics of the cancellous bone microstructure provide information that is useful to understand at a cell level the complex biological interactions and mechanisms taking place during the process of remodelling and various bone disease, e.g., osteoporosis [26]. Therefore, an effective application of the DSI method in microstructural measurements of bone tissue mechanical properties becomes crucial.

Examination of in the progress of osteoarthritis of a hip joint the selected micromechanical properties of a cancellous bone change was carried out [28]. Performed indentation tests allowed the authors to measure the characteristic parameters of hardness ($H_V$) and elasticity ($E_{IT}$) of the tissues affected by the disease. During the additional evaluation of the degree of bone mineralization (Raman analysis) and of density changes (μCT), the conclusions concerning the source of changes in the structure of the bones in arthrosis (AO) were formulated.

The indentation method was used not only to measure the parameters of hardness and elasticity at the micro level, but also to determine the properties and coefficients related to the viscoelasticity [7], [22], cracking, creep and relaxation [30].

In many works the authors emphasize that the important factors influencing the measurement are: the quality and the way of preparation of the sample, the state of humidity of the sample, thermal conditions of the test, stiffness of the measurement system, the type and the condition of the indenter, as well as the process parameters, i.e., the value of the force, velocity and time of sample loading [13], [28].

The chief aim of the studies presented in the paper is to determine the influence of the DSI test conditions, i.e., force rate, constant pick force time and maximal force value, on selected mechanical properties of a trabecular bone tissue. During the DSI tests hardness and elastic modulus of a trabecular bone tissue were measured. Also, an analysis of deformation energy curves for various test conditions is presented in this paper. The analysis comprises the determination of the ability of the material to use a strengthening phenomenon.

This type of comprehensive research and analysis performed on human preparations at different pa-

rameters of the nanoindentation process will complement the existing knowledge about the mechanical properties of bone structures at the level of microstructure. Entering into the subject of energy in the DSI method and the strengthening in reference to hard, porous tissues on the basis of the DSI method makes the undertaken research original.

# 2. Material and methods

## 2.1. Models of penetrators and their field of contact

The analytical solution for an elastic contact when pressing an axially-symmetric penetrator into a half-space was presented by Sneddon in his fundamental work [24] based on Boussinesqu's earlier approach. As a result, he obtained simple relations: the loading force ($P$) – the depth of penetration ($h$) for a wide variety of penetrator shapes – for spherical, conical shapes. These relations are expressed in the form of a power law:

$$P(h) = CEh^n, \tag{2.1}$$

where: $E$ – Young's modulus, $C$ – coefficient, $n$ – work hardening exponent

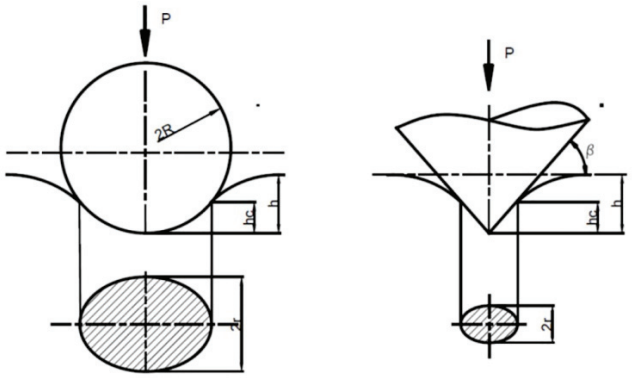


Fig. 1. Diagram presenting pressing the spherical indenter (a), conical indenter (b), by the force $P$ into an elastic half-space – the geometry of the penetrators $\beta$, $R$ and the characteristic values, i.e., penetration depth $h$, the relevant dimensions of the projection of the contact radius $r$

Geometric models and their characteristic values are shown in Fig. 1 based on the interpretation of Sakai [23]. An important parameter in the description of the mechanics of contact are the mentioned depths related to the field of direct contact (projection) $A_c$, which can be expressed for the flat penetrator, the spherical penetrator and the conical penetrator, respectively:

$$A_{c,s} = \pi r^2, \quad A_{c,c} = \pi r^2 = g h_c^2 = (\pi cot^2\beta) h_c^2. \tag{2.2}$$

An important relation, as shown in Fig. 1, is a linear correlation of the penetrator hollow depth ($h$) and the depth of contact ($h_c$), i.e.:

$$h = \gamma h_c, \tag{2.3}$$

where the coefficient takes the values $\gamma_s = 2$; $\gamma_c = \pi/2$, for the spherical penetrator, the conical penetrator, respectively.

Geometric and material characteristics described by the coefficient $C$ for the models of spherical and conical penetrators is expressed as follows:

$$C_s = \frac{4R}{3(1-\nu^2)}\left(\frac{2}{h/h_c}\right)^{3/2},$$

$$C_c = \frac{\mathrm{tg}\,\beta}{2(1-\nu^2)}\frac{\pi cot^2\beta}{(h/h_c)^2}. \tag{2.4}$$

Reflections on the analytical solution of an elastic contact of an axially-symmetric penetrator can be easily used to formulate the constitutive equation. Thus, the conversion from the space of force-penetration depth $P$–$h$ to the space of average values of stress–strain, can be made according to Johnson et al. [12].

## 2.2. Deformation work in the penetration process

Assuming that the dependence of the force on the penetration depth is described by the following equation (2.1), where the index exponent for the case of the spherical or conical penetrator can be assumed as $n = 2$ (the power law has the form $\sigma = E\varepsilon^n$), thus:

$$P = CEh^2. \tag{2.5}$$

Cheng et al. Let [2] introduced the concept of a scaling function, which can be interpreted as a dimensionless function:

$$C = C\left(\nu, n\beta, \frac{\sigma_Y}{E}\right), \tag{2.6}$$

where: $\sigma = \sigma_Y$ (limit value of elastic strains), dependent on four parameters (independent variables), which will be used in the further proceedings.

In the process of indentation during loading by the maximum (total) work used during deformation by the penetrator, it can be noted:

$$W_{tot} = \int_0^{h=h_{\max}} P \cdot dh = \int_0^{h_{\max}} C_L\left(v, n, \beta, \frac{\sigma_Y}{E}\right) E h^2 dh, \quad (2.7)$$

$$W_{tot} = C_L\left(v, n, \beta, \frac{\sigma_Y}{E}\right) E h_{\max}^3, \quad (2.8)$$

where $C_L$ – the scaling function in the process of loading.

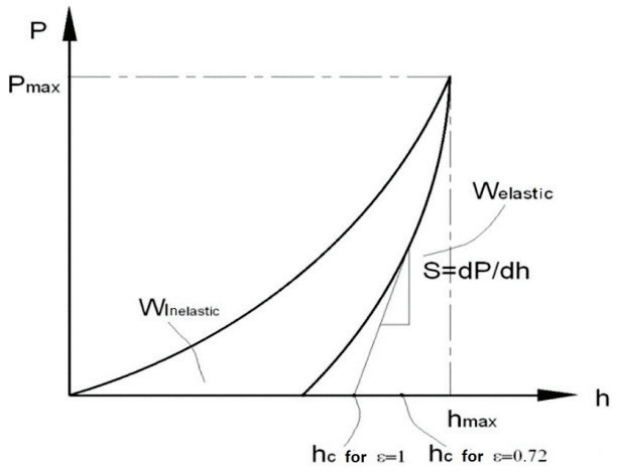


Fig. 2. Dependence of the load $P$ on the depth $h$ in the penetration process

The unloading process which is typical in the DSI processes (Fig. 2), can be determined by the equation work:

$$W_{unl} = \int_{h=h_f}^{h_{\max}} P dh = C_u\left(v, n, \beta, \frac{\sigma_Y}{E}\right) E h_{\max}^3, \quad (2.9)$$

where the final depth after unloading, as shown in Fig. 2, is determined from the condition:

$$P = 0 = E h^2 C\left(v, n, \beta, \frac{\sigma_Y}{E}, \frac{h_f}{h_{\max}}\right) \quad (2.10)$$

by the scaling function of five variables.

The relative work of unloading in the indentation process (*IT*) is interesting because of the significant correlation with the values measured by the DSI method, which include, among others, the modulus $E_{IT}$ and the hardness of the center $H_{IT}$ [18], [24], i.e.:

$$\frac{W_{tot} - W_{unl}}{W_{tot}} = 1 - k\frac{C_u\left(v, n, \beta, \frac{\sigma_Y}{E}\right)}{C_L\left(v, n, \beta, \frac{\sigma_Y}{E}\right)} = 1 - k\frac{H_{IT}}{E_{IT}}, \quad (2.11)$$

where:

$k$ – the factor that interprets the ability of the center to deform (or to strengthen [18]),

$C_u$, $C_L$ – the scaling functions,

$H_{IT}$, $E_{IT}$ – respectively indentation hardness, modulus of elasticity.

Energetic parameters for different conditions of the deformation process in the DSI research were determined on the basis of the measurements of microhardness ($H_{IT}$, $H_V$, $H_M$) and elasticity ($E_{IT}$), which were carried out with the use of Micro Hardness Tester MHT (CSEM Instruments Company) with the Vickers indenter.

## 2.3. Materials

A patient qualified for a hip replacement surgery had a femoral head routinely resected. With the approval of the Bioethics Committee of the Military Medical Institute, the specimen taken could be used for the studies of biomechanical properties of bone tissues. Figure 3 shows the method and the place of cutting the test specimen. Preparation of the samples was done in a mechanical way by cutting the specimen with the dimensions of 25 × 25 × 20 mm by a precision cutter in the axial and lateral directions of a femoral head (Fig. 4a). The following cutting pa-

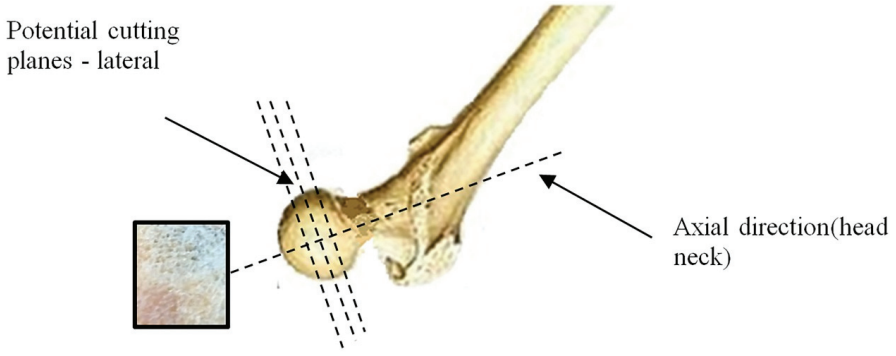


Fig. 3. A diagram showing the method of cutting the sample from the preparation according to the femoral bone anatomical planes

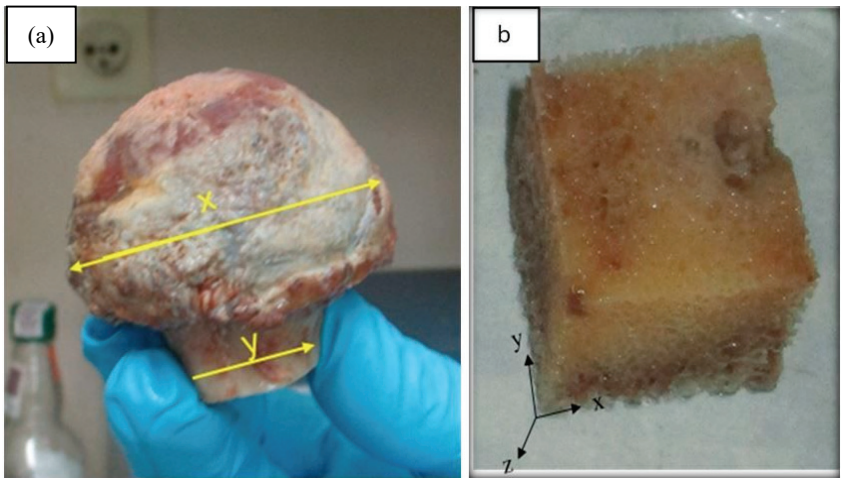


Fig. 4. Characteristic dimensions of the human femoral bone head $x = \varnothing$ 50 mm; $y = \varnothing$ 28 mm (a), the rectangular sample of the cancellous tissue of the dimensions: $x$, $y$, $z$ (25 × 25 × 20 mm) (b)

rameters were used: rotations of a dial $n$ = 3300 rpm, feed $p$ = 0.170 mm/s, while there was assumed a range of material hardness for cutting 70–400 HV, which determined the selection of an appropriate dial.

The samples (Fig. 4b) between the DSI tests were stored in a refrigerator at the temperature of 5 °C, in the solution of ethanol, in tightly closed containers.

# 3. Results and discussion

## 3.1. Study of the influence of the DSI method parameters on the hardness and elasticity of the cortical bone and cancellous bone

### 3.1.1. Study of the influence of the velocity *v* change

The first series of tests was carried out for the cancellous tissue at the constant load of 500 mN and the shifting loading rate of 5000, 10 000, 20 000, 30 000, 35 000 mN/min, and the hold time of 20 s. The measurements were repeated many times in different places of the tissue sample of the symbol *2.L62.KB.Sb.VIII15.A* (preparation no. 2, 62-year-old patient, sex: female, area: hip, Sb – cancellous structure – trabecula, date of the collection: 08.2015, sample no. from the preparation: A) on the surface *a*, i.e. perpendicular to the axial direction of the femoral head neck, in the central region of the trabecula (Fig. 5).

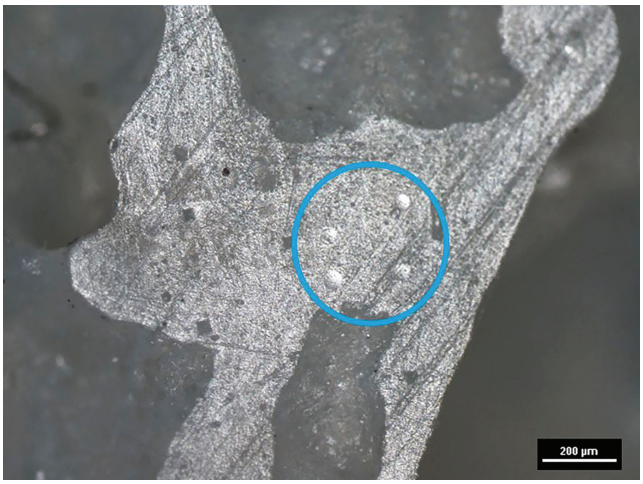


Fig. 5. Microscopic view of the bone trabecula in the sample *2.L62.KB.Sb.VIII15.A* with the selected exemplary place of the measurement in the study of indentation

Table 1. Comparison of the mean values including the standard deviation measurements for the microhardness and elasticity of a trabecular bone; $\tau$ = 20 s, $P_{max}$ = 500 mN

| Parameter | $v$ = 5000 mN/min | $v$ = 10 000 mN/min | $v$ = 20 000 mN/min | $v$ = 30 000 mN/min | $v$ = 35 000 mN/min |
|---|---|---|---|---|---|
| $H_{IT}$ | 301.06 ± 61.45 | 292.58 ± 39.13 | 318.80 ± 34.59 | 357.68 ± 42.79 | 279.40 ± 59.56 |
| $H_M$ | 195.37 ± 43.36 | 174.69 ± 30.32 | 205.02 ± 19.78 | 238.60 ± 36.07 | 171.60 ± 47.36 |
| $H_V$ | 28.42 ± 5.80 | 27.61 ± 3.69 | 30.09 ± 3.26 | 33.76 ± 4.04 | 26.37 ± 5.62 |
| $E_{IT}$ | 4.64 ± 1.29 | 3.85 ± 1.46 | 4.62 ± 0.54 | 5.69 ± 1.39 | 3.55 ± 1.47 |

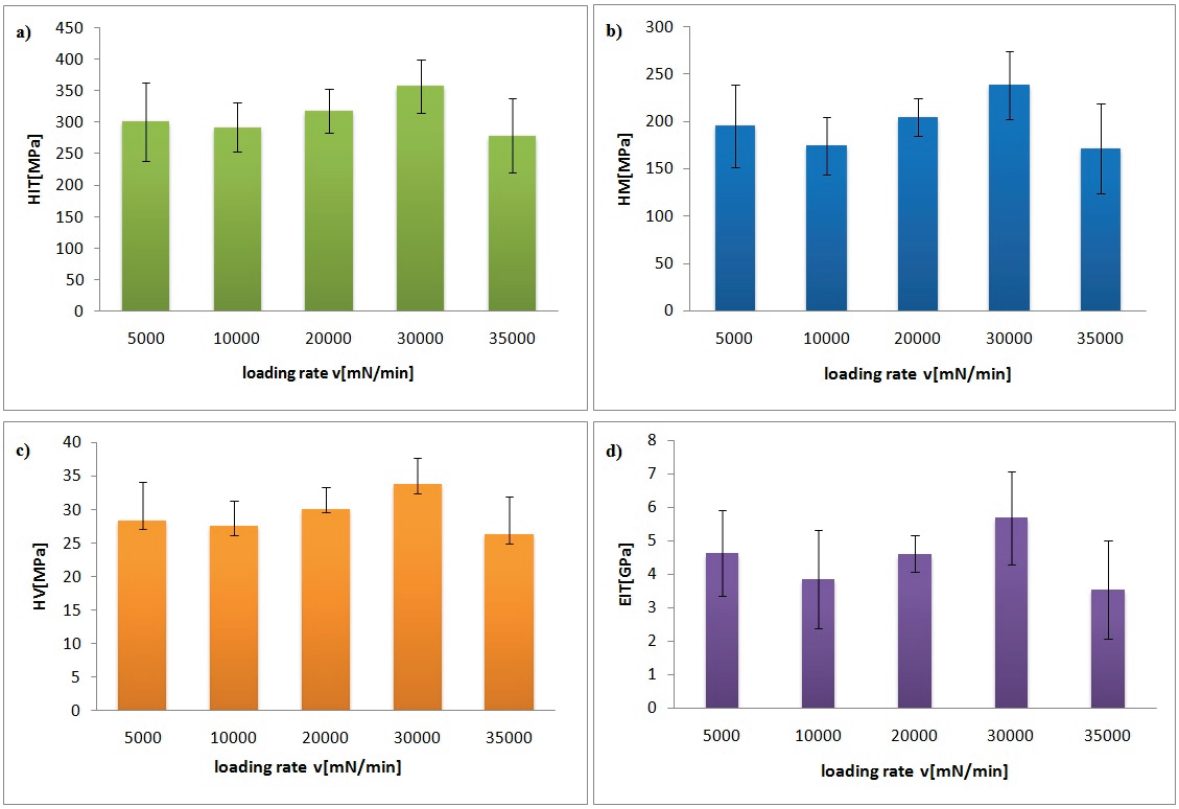


Fig. 6. Comparison of the average values of hardness $H_{IT}$ [MPa] (a), $H_M$ [MPa] (b), $H_V$ [MPa] (c) and the elastic modulus $E_{IT}$ [GPa] (d) for a trabecular bone; $\tau = 20$ s, $P_{max} = 500$ mN at different loading velocities

Table 1 presents the results of the measurements of microhardness $H_v$ (classical measurement), $H_M$ and $H_{IT}$ and $E_{IT}$ for the series of 7 measurements performed in the above-mentioned conditions The adopted velocities correspond to the literature research [6] carried out for another material with a non-linear viscoelastic properties, i.e., of Cheddar cheese.

The measurements were performed under the controlled environmental conditions (temperature of 20 ± 0.5 °C, air humidity 32 ± 5%).

The figures 6a–c show in the measurement of the indentation the dependence of the average value of microhardness on the loading rate at the constant hold time and the maximum loading force, based on the measurement of indentation. Similarly to the studies of hardness, the influence of the measurement conditions on the elastic properties of the tissues was evaluated. The bar graph in Fig. 6d reveals these studies.

### 3.1.2. Study of the influence of the hold time $\tau$ change

In order to determine the influence of the hold time on the studied material properties of the tissues, a series of studies was performed for the cancellous tissue at the constant load of 500 mN, the constant loading rate of 600 mN/min, and the variable hold time of 0.1, 1, 10, 100 and 1000 sec. As previously, the measurements were repeated several times at different places of the tissue sample number 1 in the area of the trabecula.

Table 2 presents the measurement results of microhardness $H_V$, $H_M$ and $H_{IT}$ and $E_{IT}$ for the series of

Table 2. Comparison of the mean values including the standard deviation measurements for the microhardness and elasticity of a trabecular bone; $P_{max} = 500$ mN, $v = 600$ mN/min

| Parameter | $\tau = 0.1$ s | $\tau = 1$ s | $\tau = 10$ s | $\tau = 100$ s | $\tau = 1000$ s |
|---|---|---|---|---|---|
| $H_{IT}$ | 418.89 ± 34.32 | 390.46 ± 50.25 | 312.97 ± 53.60 | 305.41 ± 53.76 | 276.23 ± 90.40 |
| $H_M$ | 287.55 ± 27.63 | 276.62 ± 38.02 | 227.15 ± 36.42 | 223.69 ± 36.66 | 199.39 ± 62.82 |
| $H_V$ | 39.54 ± 3.24 | 36.85 ± 4.74 | 29.54 ± 5.06 | 28.83 ± 5.07 | 26.07 ± 8.53 |
| $E_{IT}$ | 7.70 ± 1.24 | 8.01 ± 1.54 | 7.01 ± 0.99 | 7.22 ± 0.97 | 6.23 ± 1.83 |

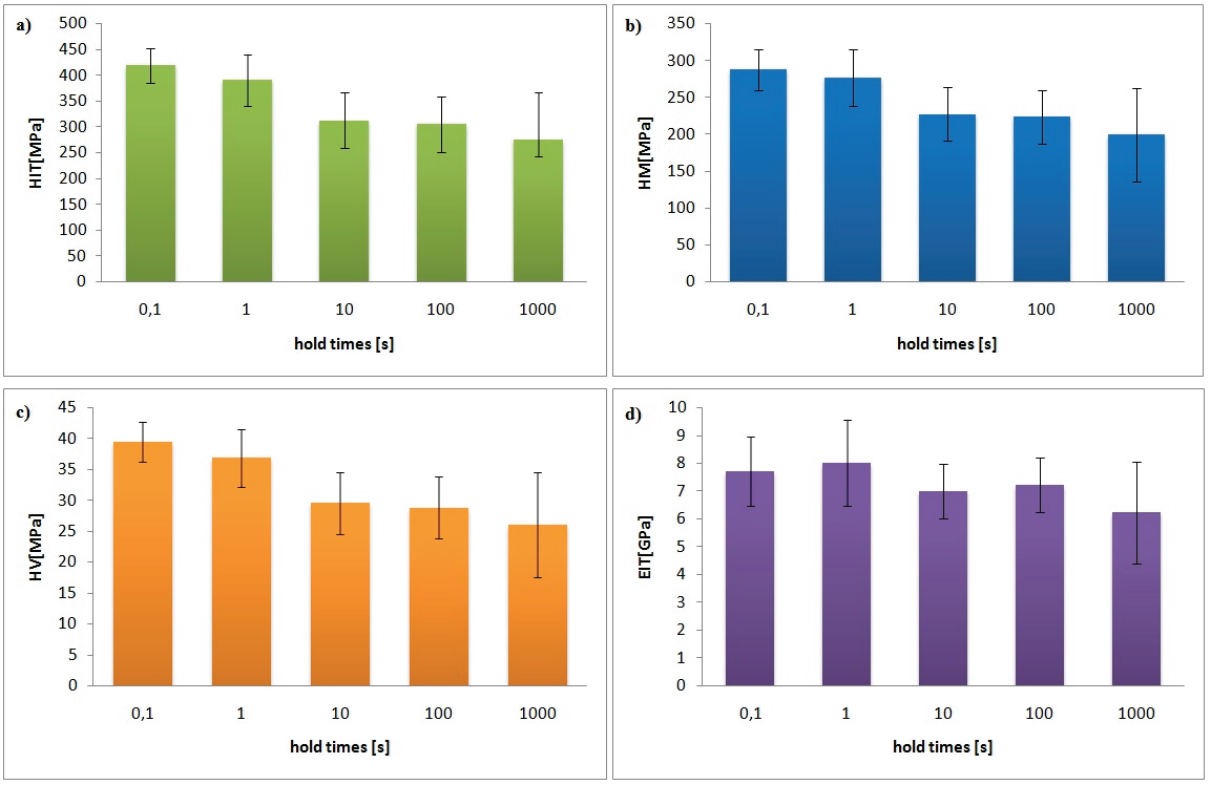


Fig. 7. Comparison of the average values of hardness $H_{IT}$ [MPa] (a), $H_M$ [MPa] (b), $H_V$ [MPa] (c), and the elastic modulus $E_{IT}$ [GPa] (d) for a trabecular bone; $P_{max}$ = 500 mN, $v$ = 600 mN/min at different hold times

7 measurements performed in different places of indentation and are presented in the Figs. 7a–d. The measurements were performed in a controlled environment (temperature of 20 ± 0.5 °C, air humidity of 32 ± 5%).

### 3.1.3. Study of the influence of the maximum loading force $P_{max}$ change

The last series of tests was carried out for the cancellous tissue at the constant hold time $\tau$ = 20 sec and the constant loading rate of 600 mN/min. The variable maximum loading/unloading force was tested. The measurements were repeated several times at different places of the tissue sample number 1 in the area of the trabecula.

Table 3 presents the measurement results of microhardness $H_v$, $H_M$ and $H_{IT}$ and $E_{IT}$ for the series of 7 measurements performed in the above-mentioned conditions. The varying values of maximum loading/unloading force $P_{max}$ were tested, i.e., 300, 500 and 600 mN.

The measurements were performed in the controlled environment (temperature of 20 ± 0.5 °C, air humidity of 32 ± 5%). The relevant comparison of the average values of hardness and elasticity are presented in Table 3 and in bar charts Figs. 8a–8d.

Table 3. Comparison of the average values including the standard deviation measurements| for the microhardness and elasticity of the trabecular bone at $v$ = 600 mN/ min, $\tau$ = 20 s and different values of the maximum loading/unloading force $P_{max}$

| Parameter | $P_{max}$ = 300 mN | $P_{max}$ = 500 mN | $P_{max}$ = 600 nM |
|---|---|---|---|
| $H_{IT}$ | 734.74 ± 46.77 | 805.24 ± 22.36 | 583.68 ± 59.50 |
| $H_M$ | 552.00 ± 45.94 | 627.72 ± 19.93 | 421.94 ± 43.46 |
| $H_V$ | 69.35 ± 4.41 | 76.00 ± 2.11 | 55.09 ± 5.62 |
| $E_{IT}$ | 19.64 ± 3.56 | 26.26 ± 1.66 | 12.90 ± 1.58 |

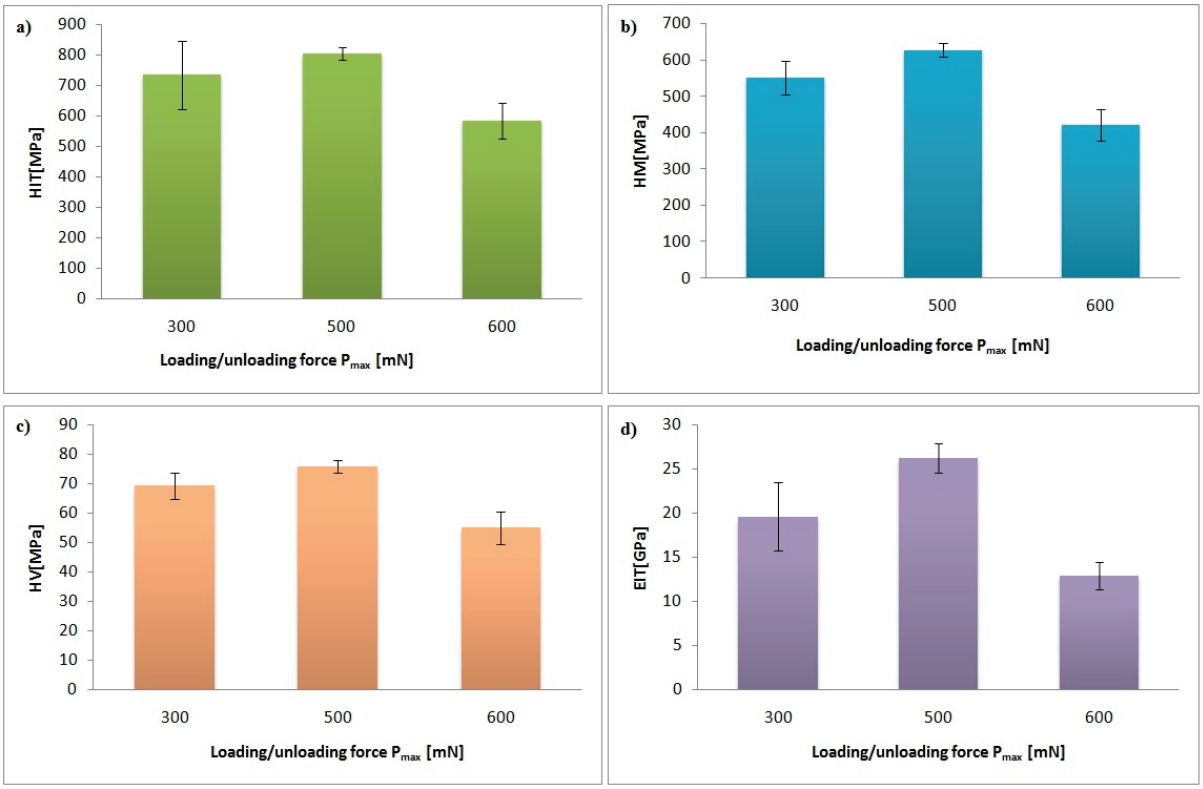


Fig. 8. Comparison of average values of $H_{IT}$ [MPa] (a), $H_M$ [MPa] (b) $H_V$ [MPa] (c) and of $E_{IT}$ [MPa] (d), for the trabecular bone: $v$ = 600 mN/min, $\tau$ = 20 s at different values of maximum loading/unloading force $P_{max}$

## 3.2. Analysis of the deformation energy curves for various conditions of the processes

The *P-h* curves registered in the studies by means of the DSI method include the process of loading (to the maximum values $P_{max}$ – $h_{max}$) and total unloading. In order to specify the ability of a bone tissue to accumulate the total energy (inelastic work) of the material deformation, the area under the curve *P–h* – $W_{inelastic}$ was determined by the integration method. The total energy $W_{total}$ was determined (Fig. 2). The difference of these values gives the information about an elastic response of the material to the process of the indenter getting into the material, i.e., $W_{elastic}$.

Knowing the parameters of hardness and elasticity as well as a relative measure of the deformation energy (determined by the difference between the total energy and the elastic energy), it is possible to estimate (according to formula (3.1)) the constant $k$, which is thought to be a measure of the ability of a material to strengthen:

$$\frac{W_{tot.} - W_{elast.}}{W_{tot.}} = 1 - k\frac{H}{E}, \quad k - \text{material factor}. \quad (3.1)$$

Tables 4–6 and in Figs. 9–14 summarize the average values of energy parameters $W_{inelastic}$, $W_{total}$, $W_{elastic}$ and the coefficient $k$ for various process conditions, i.e.:

- at the variable velocity $v$ (loading/unloading), the constant hold time $\tau$ and the constant maximum loading force $P_{max}$;

Table 4. Determination of the hysteresis fields of the loading/unloading curves and the coefficient $k$ of the potential evaluation of the ability of a material to strengthen for the trabecular bone at different loading rate of the sample; $\tau$ = 20 s, $P_{max}$ = 500 mN

| Parameter | $v$ = 5000 mN/min | $v$ = 10000 mN/min | $v$ = 20000 mN/min | $v$ = 30000 mN/min | $v$ = 35000 mN/min |
|---|---|---|---|---|---|
| $W_{inlast}$ [Nm] | $1.62{\cdot}10^{-6} \pm 2.6{\cdot}10^{-7}$ | $1.63{\cdot}10^{-6} \pm 1.4{\cdot}10^{-7}$ | $1.71{\cdot}10^{-6} \pm 1.2{\cdot}10^{-7}$ | $1.76{\cdot}10^{-6} \pm 1.7{\cdot}10^{-7}$ | $2.07{\cdot}10^{-6} \pm 3.4{\cdot}10^{-7}$ |
| $W_{elast}$ [Nm] | $6.70{\cdot}10^{-7} \pm 9.3{\cdot}10^{-8}$ | $9.62{\cdot}10^{-7} \pm 1.2{\cdot}10^{-8}$ | $7.37{\cdot}10^{-7} \pm 1.9{\cdot}10^{-8}$ | $7.22{\cdot}10^{-7} \pm 6.3{\cdot}10^{-8}$ | $1.20{\cdot}10^{-6} \pm 3.4{\cdot}10^{-7}$ |
| $W_{tot}$ [Nm] | $2.29{\cdot}10^{-6} \pm 3.6{\cdot}10^{-7}$ | $2.59{\cdot}10^{-6} \pm 2.6{\cdot}10^{-7}$ | $2.44{\cdot}10^{-6} \pm 1.4{\cdot}10^{-7}$ | $2.48{\cdot}10^{-6} \pm 2.4{\cdot}10^{-7}$ | $3.27{\cdot}10^{-6} \pm 6.8{\cdot}10^{-7}$ |
| $k$ [–] | 4.45 ± 0.43 | 4.55 ± 0.98 | 4.31 ± 0.29 | 4.45 ± 0.38 | 4.30 ± 0.55 |

Table 5. Determination of the hysteresis fields of the loading/unloading curves and the coefficient $k$ of the potential evaluation of the ability of a material to strengthen for the trabecular bone at different hold time of the indenter; $P_{max} = 500$ mN, $v = 600$ mN/min

| Parameter | $\tau = 0.1$ s | $\tau = 1$ s | $\tau = 10$ s | $\tau = 100$ s | $\tau = 1000$ s |
|---|---|---|---|---|---|
| $W_{inlast}$ [Nm] | $1.05 \cdot 10^{-6} \pm 1.2 \cdot 10^{-7}$ | $1.07 \cdot 10^{-6} \pm 7.6 \cdot 10^{-8}$ | $1.26 \cdot 10^{-6} \pm 1.9 \cdot 10^{-7}$ | $1.56 \cdot 10^{-6} \pm 1.9 \cdot 10^{-7}$ | $1.67 \cdot 10^{-6} \pm 2.6 \cdot 10^{-7}$ |
| $W_{elast}$ [Nm] | $4.11 \cdot 10^{-7} \pm 4.2 \cdot 10^{-8}$ | $4.12 \cdot 10^{-7} \pm 6.4 \cdot 10^{-8}$ | $4.71 \cdot 10^{-7} \pm 6.0 \cdot 10^{-9}$ | $4.33 \cdot 10^{-7} \pm 5.5 \cdot 10^{-9}$ | $5.11 \cdot 10^{-7} \pm 7.4 \cdot 10^{-8}$ |
| $W_{tot}$ [Nm] | $1.46 \cdot 10^{-6} \pm 1.6 \cdot 10^{-7}$ | $1.48 \cdot 10^{-6} \pm 1.4 \cdot 10^{-7}$ | $1.74 \cdot 10^{-6} \pm 1.9 \cdot 10^{-7}$ | $1.99 \cdot 10^{-6} \pm 1.9 \cdot 10^{-7}$ | $2.18 \cdot 10^{-6} \pm 3.3 \cdot 10^{-7}$ |
| $k$ [–] | $5.10 \pm 0.52$ | $5.61 \pm 0.33$ | $6.12 \pm 0.26$ | $5.22 \pm 0.76$ | $5.37 \pm 0.67$ |

Table 6. Determination of the hysteresis fields of the loading/unloading curves and the coefficient $k$ of the potential evaluation of the ability of a material to strengthen for the trabecular bone at different maximum loading/unloading force; $v = 600$ mN/min, $\tau = 20$ s

| Parameter | $P_{max} = 300$ mN | $P_{max} = 500$ mN | $P_{max} = 600$ nM |
|---|---|---|---|
| $W_{inlast}$ [Nm] | $4.26 \cdot 10^{-7} \pm 2.0 \cdot 10^{-8}$ | $8.67 \cdot 10^{-7} \pm 2.2 \cdot 10^{-8}$ | $1.27 \cdot 10^{-6} \pm 7.2 \cdot 10^{-8}$ |
| $W_{elast}$ [Nm] | $1.14 \cdot 10^{-7} \pm 1.2 \cdot 10^{-8}$ | $1.89 \cdot 10^{-7} \pm 9 \cdot 10^{-10}$ | $4.45 \cdot 10^{-7} \pm 3.1 \cdot 10^{-8}$ |
| $W_{tot}$ [Nm] | $5.40 \cdot 10^{-7} \pm 3.2 \cdot 10^{-8}$ | $1.06 \cdot 10^{-6} \pm 2 \cdot 10^{-8}$ | $1.71 \cdot 10^{-6} \pm 1.0 \cdot 10^{-7}$ |
| $k$ [–] | $6.24 \pm 0.93$ | $5.83 \pm 0.22$ | $5.72 \pm 0.17$ |

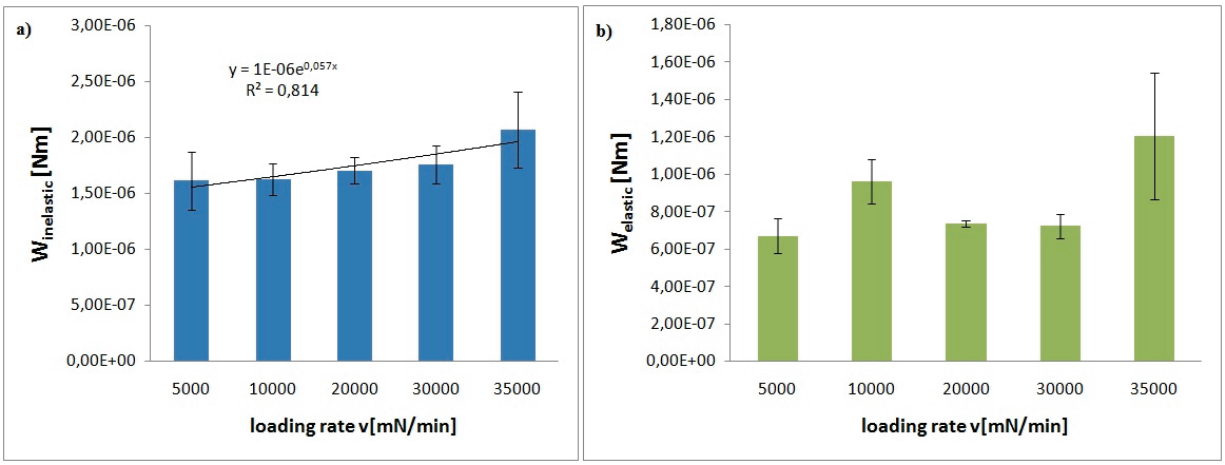


Fig. 9. Comparison of the inelastic (a) and elastic (b) deformation work for the trabecular bone in an indentation test performed at different loading/unloading rate

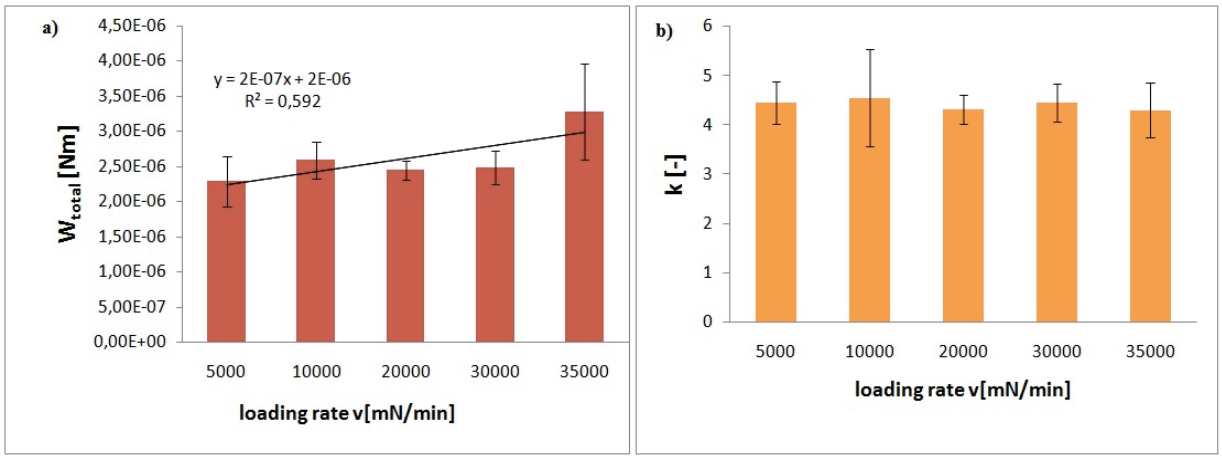


Fig. 10. Comparison of the average total work (a) and of the average coefficient $k$ (b) for the trabecular bone in an indentation test performed at different loading/unloading rate

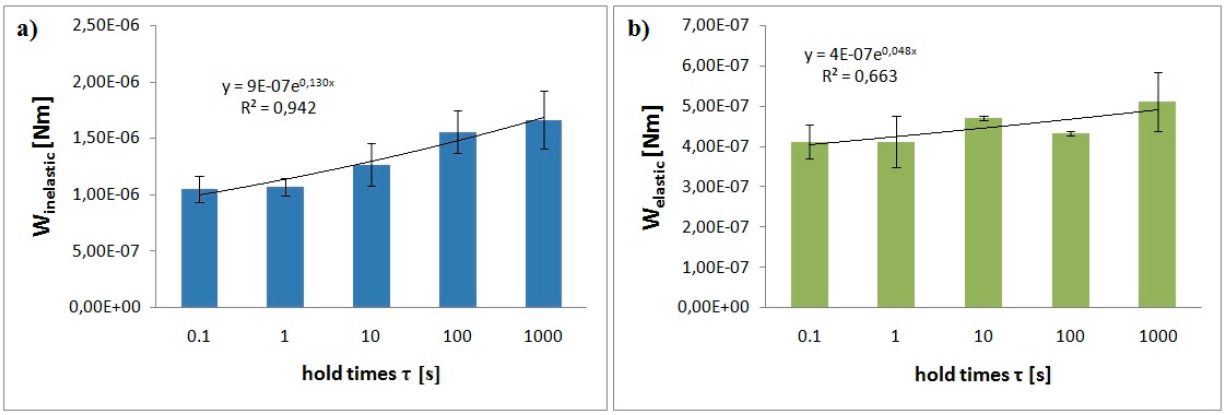


Fig. 11. Comparison of the inelastic (a) and elastic (b) deformation work
for the trabecular bone in an indentation test performed at different hold time of the indenter

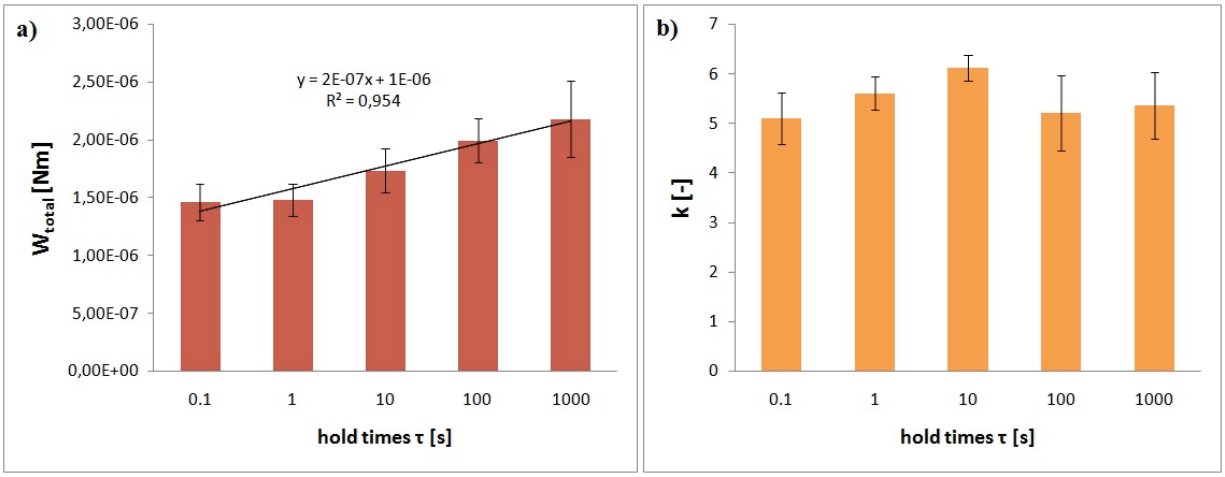


Fig. 12. Comparison of the average total work (a) and the average coefficient *k* (b)
for the trabecular bone in an indentation test performed at different hold time of the indenter

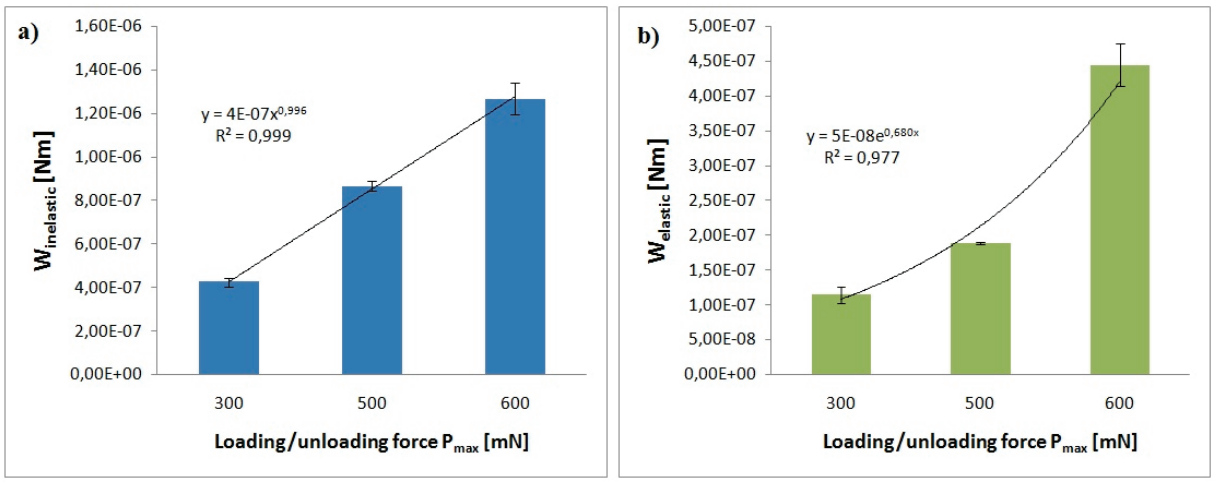


Fig. 13. Comparison of the inelastic (a) and elastic (b) deformation work
for the trabecular bone in an indentation test performed at different maximum loading/unloading force

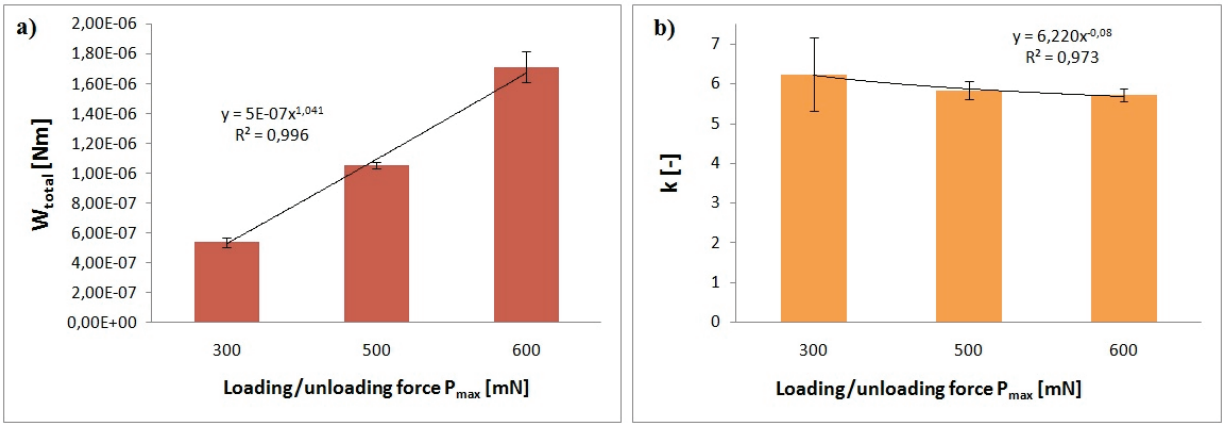


Fig. 14. Comparison of the average total work (a) and the average coefficient $k$ (b) for the trabecular bone in an indentation test performed at different maximum loading/unloading force

- at the variable hold time $\tau$, constant velocity $v$ (loading/unloading) and the constant maximum loading force $P_{max}$;
- at the variable maximum loading force $P_{max}$ and the constant: hold time $\tau$ and velocity $v$ (loading/unloading).

The schematics indicate trend lines with the best possible fit to the existing functions, i.e., linear, exponential, power, logarithmic, with a maximum correlation coefficient $R^2$.

Summarizing, it is possible to state (on the basis of the charts 9a, 10d, 11a, 12a, and 13a–14b, in which trend lines are marked) that the potential tendency of strengthening/weakening of the tissue is visible. These preliminary results shall inspire further research in this area.

# 4. Conclusions

- The analysis of the results of measurements and the calculations of total energy, i.e., elastic and inelastic ($W_{total}$, $W_{elastic}$, $W_{inelastic}$) and of the parameters of hardness ($H_V$, $H_M$, $H_{IT}$) and elasticity ($E_{IT}$) made it possible to assess the influence of the process parameters (loading rate, force and hold time) on mechanical properties of bone structures at a microscopic level.
- The coefficient $k$ dependent on the ratio $E_{IT}/H_{IT}$ and on the stored energy ($\Delta W = W_{total} - W_{elastic}$) is a measure of reaction of the material to the loading and the deformation of tissue, what can be seen in Figs. 10b, 12b and 14b.
- In the conducted research one could observe a noticeable influence of the parameters, such as: loading/unloading rate, hold time, and the value of the maximum loading force on the parameters of hardness and elasticity of the bone tissue, in particular, the cancellous bone:
  - in the lower range the increase of loading/unloading velocity is associated with the increase of $E_{IT}$ coupled with the reduction of the inelastic material reaction (decrease of $W_{inelastic}$ and $W_{total}$), while in high-velocity tests (5000–35000 mN/min), the opposite trend was observed, i.e., the increase of deformation ($W_{inelastic}$) along with the increase of velocity;
  - the increase of hold time is associated with the decrease of hardness parameters $H_{IT}$, $H_V$ and elasticity $E_{IT}$, as well as with the increase of the elastic and inelastic reaction of material ($W_{inelastic}$, $W_{eleastic}$ and $W_{total}$).
  - the increase of the maximum loading/unloading force does not influence in any significant way the change in the parameters of hardness and elasticity, however, it is reflected in the increase of the reaction of inelastic and elastic bone structure in response to the increase of the load, as indicated by the force curve analysis.
- Shortening of the hold time is reflected in the reduction of the hysteresis field. The shorter hold time also results in a smaller indentation depth obtained with the same loading/unloading force and velocity.
- The increase of loading/unloading rate is associated with the reduction of the hysteresis field. The lower velocity results in a greater depth of indentation when using the same force.
- It was observed that there was a slight influence of the test parameters: $v$, $\tau$, $P_{max}$ on the coefficient $k$ postulated as a measure of the tendency to strengthen. At lower velocities, it was possible to observe a slight increase in the coefficient val-

ues with an increase of $v$, while there was an opposite trend with increasing the maximum loading/unloading force $P_{max}$. Changes in the average value of the coefficient are slight (they are contained in the range of 4.3 to 6.24), therefore, it is possible to formulate careful conclusions about the universality of the coefficient $k$ as a constant characterizing the materials ability to strengthen, not only with respect to tissue structures. However, further studies are needed, in particular, the implementation of similar analyses of energy curves for the materials with different characteristics (super-hard and soft).

- In the carried out tests the insertion of the indenter into the trabecula (made up of concentrically arranged bone lamellae) occurred to the depth of from 4 to 11 μm (depending on the test parameters). The thickness of the individual bone plate (lamella) is 2–4 microns. Thus, when the indenter was moved in an axis perpendicular to the plane of the section of osteon, the elastic and inelastic (plastic viscoelastic) deformation occurred in an axial direction of a single bone lamella formed by the elastic collagen fibers which were arranged spirally and reinforced with hydroxyapatite. However, when the insertion occurred in a direction parallel to the plane of the section, probably the compression and the deformation of several bone lamellae, which acted as a composite of the type of sandwich, occurred. Consequently, depending on the loading direction the material reaction will vary. With loading of a single lamella, the elastic deformation and the energy absorption, due to the viscoelastic properties of the material, occur at the first stage. In the second case under consideration, some micro-cracks of the lamellae may occur, which could explain an increase in energy parameters – the work of elastic and inelastic deformation, and the total work at higher loading/unloading force, longer retention time and higher velocities. The lower value of the parameter $k$ is obtained for hard materials (e.g., SiC, $ZnO_2$), and therefore the decline in the value of this parameter with the increase of $v$, $\tau$, $P_{max}$, induces to further research on the potential ability of a bone tissue to strengthen and the nature of this phenomenon.
- The characteristics of the mechanical properties of bone tissues provide some useful information to understand the complex interactions of biological and cellular mechanisms that occur during the remodeling as well as in bone diseases (e.g., osteoporosis). It will also serve the practical use of this data in the design of biocompatible materials and applications in arthroplasty and in a rehabilitation procedure of such diseases as osteoporosis.
- It should be emphasized that the research carried out on human preparations yields additional information on the dependence of mechanical properties of bone microstructures on nanoindentation process parameters. An attempt to assess the biological material, which is a porous structure, by testing its ability to strengthen, in particular, on the basis of the energy aspects, the parameters of hardness and elasticity is also innovative.

## Acknowledgements

The study was supported by the Ministry of Science and Higher Education – the research project National Science Centre (NCN) No. 2014/15/B/ST7/03244.

## References

[1] CHENG Y.T., CHENG C.M., *Relationships between initial unloading slope, contact depth, and mechanical properties for conical indentation in linear viscoelastic solids*, J. Mater. Res., 2005, 20, 1046–1053.

[2] CHENG Y.T., CHENG C.M., *Relationships between hardness, elastic modulus, and the work of indentation*, Appl. Phys. Lett., 1998, 73(5), 614–616.

[3] COUTTS L.V., JENKINS T., LI T., DUNLOP D.G., OREFFO R.O., COOPER C., HARVEY N.C., THURNER P.J., *Variability in reference point microindentation and recommendations for testing cortical bone: Location, thickness and orientation heterogeneity*, J. Mech. Behav. Biomed. Mater., 2015, 46, 292–304.

[4] COWIN S.C., DOTY S.B., *Tissue Mechanics*, Springer, 2007.

[5] DALL'ARA E., GRABOWSKI P., ZIOUPOS P., VICECONTI M., *Estimation of local anisotropy of plexiform bone: Comparison between depth sensing micro-indentation and Reference Point Indentation*, J. Biomech., 2015, 48, 4073–4080.

[6] DEMIRAL M., ABDEL-WAHAB A., SILBERSCHMIDT V., *A numerical study on indentation properties of cortical bone tissue: Influence of anisotropy*, Acta Bioeng. Biomech., 2015, 17(2), 3–14.

[7] DEMIRCI N., TÖNÜK E., *Non-integer viscoelastic constitutive law to model soft biological tissues to in-vivo indentation*, Acta Bioeng. Biomech., 2014, 16(4), 13–21.

[8] GIBSON R.F., *A review of recent research on nanoindentation of polymer composites and their constituents*, Compos. Sci. Technol., 2014, 105, 51–65.

[9] GOH S.M., CHARALAMBIDES M.N., WILLIAMS J.G., *Indentation testing of mild cheddar cheese*, J. Texture. Stud., 2005, 36, 459–477.

[10] BUCAILLE J.L., STAUSS S., FELDER E., MICHLER J., *Determination of plastic properties of metals by instrumented indentation using different sharp indenters*, Acta Mater., 2003, 51, 1663–1678.

[11] JENKINS T., COUTTS L.V., DUNLOP D.G., OREFFO R.O., COOPER C., HARVEY N.C., THURNER P.J., *Variability in ref-*

*erence point microindentation and recommendations for testing cortical bone: Maximum load, sample orientation, mode of use, sample preparation and measurement sparing*, J. Mech. Behav. Biomed. Mater., 2015, 42, 311–324.

[12] JOHNSON K.L., *Contact Mechanics*, Cambridge Univ. Press, 1985.

[13] JOHNSON W.M., RAPOFF A.J., *Microindentation in bone: Hardness variation with five independent variables*, J. Mater. Sci. – Mater. M., 2007, 18, 591–597.

[14] KATSAMENIS O.L., JENKINS T., THURNER P.J., *Toughness and damage susceptibility in human cortical bone is proportional to mechanical in homogeneity at the osteonal-level*, Bone, 2015, 76, 158–168.

[15] KOKOT G., *Wyznaczanie własności mechanicznych tkanek kostnych z zastosowaniem cyfrowej korelacji obrazu, nanoindentacji oraz symulacji numerycznych*, Wydaw. Politech. Śl., 2013.

[16] LITNIEWSKI J., *Determination of the elasticity coefficient for a single trabecula of a cancellous bone: Scanning Acoustic Microscopy approach*, Ultrasound Med. Biol., 2005, 31(10), 1361–1366.

[17] OLIVEIRA G.L., COSTA C.A., TEIXEIRA S.C.S., COSTA M.F., *The use of nano- and micro-instrumented indentation tests to evaluate viscoelastic behavior of poly(vinylidene fluoride) (PVDF)*, Polym. Test., 2014, 34, 10–16.

[18] OLIVER W.C., PHARR G.M., *Measurement of hardness and elastic modulus by instrumented indentation: Advances in understanding and refinements to methodology*, J. Mater. Res., 2004, 19(1), 3–20.

[19] PN-EN ISO 14577-1: *Metale – Instrumentalna próba wciskania wgłębnika do określania twardości i innych własności materiałów* – Część 1: *Metoda badania*, PKN, 2015.

[20] POKORSKA I., SKALSKI K., MAKUCH A., PAWLIKOWSKI M., *Measurement of mechanical properties of bone tissue on microstructural level by using DSI (Depth Sensing Indentation) method*, Inż. Powierz., 2015, 1, 68–80.

[21] RHO J.Y., ROY M.E., TSUI T.Y., PHARR G.M., *Elastic properties of microstructural components of human bone tissue as measured by nanoindentation*, J. Biomed. Mater. Res., 1999, 45(1), 48–54.

[22] RODRIGUEZ-FLOREZ N., OYEN M.L., SHEFELBINE S.J., *Insight into differences in nanoindentation properties of bone*, J. Mech. Behav. Biomed. Mater., 2013, 18, 90–99.

[23] SAKAI M., *Time-dependent viscoelastic relation between load and penetration for an axisymmetric indenter*, Philos. Mag. A, 2002, 82(10), 1841–1849.

[24] SNEDDON I.N., *The relation between load and penetration in the axisymmetric boussinesq problem for a punch of arbitrary profile*, Int. J. Eng. Sci., 1965, 3(1), 47–57.

[25] SOONS J., LAVA P., DEBRUYNE D., DIRCKX J., *Full-field optical deformation measurement in biomechanics: Digital speckle pattern interferometry and 3D digital image correlation applied to bird beaks*, J. Mech. Behav. Biomed. Mater., 2012, 14, 186–191.

[26] SZTEFEK P., VANLEENE M., OLSSON R., COLLINSON R., PITSILLIDES A.A., SHEFELBINE S., *Using digital image correlation to determine bone surface strains during loading and after adaptation of the mouse tibia*, J. Biomech., 2010, 43, 599–605.

[27] TANG X.G., HOU M., TRUSS R., ZOU J., YANG W., DONG Z.G., HUANG H., *An unexpected plasticization phenomenon and a constant of the change rate of viscoelastic properties for polymers during nanoindentation test*, J. Appl. Polym. Sci., 2011, 122, 885–890.

[28] TOMANIK M., NIKODEM A., FILIPIAK J., *Microhardness of human cancellous bone tissue in progressive hip osteoarthritis*, J. Mech. Behav. Biomed. Mater., 2016, 64, 86–93.

[29] VOYIADJIS G.Z., ALMASRI A.H., PARK T., *Experimental nanoindentation of BCC metals*, Mech. Res. Commun., 2010, 37(3), 307–314.

[30] WU Z., BAKER T.A., OVAERT T.C., NIEBUR G.L., *The effect of holding time on nanoindentation measurements of creep in bone*, J. Biomech., 2011, 44, 1066–1072.